Cerebral Cortex, March 2018;28: 880–893

doi: 10.1093/cercor/bhw410
Advance Access Publication Date: 11 January 2017
Original Article

ORIGINAL ARTICLE

Medial Prefrontal Cortex–Pontine Nuclei Projections Modulate Suboptimal Cue-Induced Associative Motor Learning

Guang-Yan Wu[1,2,†], Shu-Lei Liu[1,2,†], Juan Yao[2], Lin Sun[3], Bing Wu[2], Yi Yang[2], Xuan Li[2], Qian-Quan Sun[4], Hua Feng[5] and Jian-Feng Sui[1,2]

[1]Department of Physiology, College of Basic Medical Sciences, Third Military Medical University, Chongqing 400038, China, [2]Experimental Center of Basic Medicine, College of Basic Medical Sciences, Third Military Medical University, Chongqing 400038, China, [3]Institute of Physical Education, Southwest University, Chongqing 400715, China, [4]Department of Zoology and Physiology, University of Wyoming, Laramie, WY 82071, USA and [5]Department of Neurosurgery, Southwest Hospital, Third Military Medical University, Chongqing 400038, China

Address correspondence to Jian-Feng Sui, Department of Physiology, College of Basic Medical Sciences, Third Military Medical University, Chongqing 400038, China. Email: jfsui2003@163.com; Hua Feng, Department of Neurosurgery, Southwest Hospital, Third Military Medical University, Chongqing 400038, China. Email: fenghua8888@vip.163.com.

[†]These authors contributed equally to this work.

Abstract

Diverse and powerful mechanisms have evolved to enable organisms to modulate learning and memory under a variety of survival conditions. Cumulative evidence has shown that the prefrontal cortex (PFC) is closely involved in many higher-order cognitive functions. However, when and how the medial PFC (mPFC) modulates associative motor learning remains largely unknown. Here, we show that delay eyeblink conditioning (DEC) with the weak conditioned stimulus (wCS) but not the strong CS (sCS) elicited a significant increase in the levels of c-Fos expression in caudal mPFC. Both optogenetic inhibition and activation of the bilateral caudal mPFC, or its axon terminals at the pontine nucleus (PN) contralateral to the training eye, significantly impaired the acquisition, recent and remote retrieval of DEC with the wCS but not the sCS. However, direct optogenetic activation of the contralateral PN had no significant effect on the acquisition, recent and remote retrieval of DEC. These results are of great importance in understanding the elusive role of the mPFC and its projection to PN in subserving the associative motor learning under suboptimal learning cue.

Key words: associative motor learning, medial prefrontal cortex, pontine nuclei, suboptimal cue

Introduction

Accumulating evidence suggests that the prefrontal cortex (PFC), which is constructed with the highest level of hierarchical organization in the entire neocortex, is closely involved in working memory (Allen and Fortin 2013; Liu et al. 2014; Lapish et al. 2015) and encoding and retrieval of declarative memory, including episodic and semantic memory (Lepage et al. 2000; Prince et al. 2007; Gigi et al. 2010; de Souza Silva et al. 2016). Traditional lesions and inactivation studies suggest that the mPFC may also be involved in associative motor learning/memory, including delay eyeblink conditioning (DEC) (Wu et al. 2012). However, when and how the mPFC modulates the associative motor

learning remains largely unknown. As one of the most important mechanisms for organisms to adapt to the environment, the associative motor learning requires brain to associate a relevant neutral stimulus (referred to as the conditioned stimulus, CS) with an aversive stimulus (referred to as the unconditioned stimulus, US), to produce defensive, automatic, and discrete motor responses with accurate timing and strength (Bellebaum and Daum 2011; Freeman 2015). It is generally accepted that the cerebellum comprises essential and sufficient sites for supporting an associative motor learning under optimal learning conditions (Kim et al. 1998; Christian and Thompson 2003; ten Brinke et al. 2015), but not under suboptimal conditions (Taub and Mintz 2010). However, learning conditions for associative motor learning are not always optimal in diverse environment. For survival, organisms should be capable of establishing associative motor learning under suboptimal learning conditions. Hence, contribution of the extra-cerebellar sites to facilitate associative motor learning may be necessary under these circumstances (Taub and Mintz 2010). Increasing evidence suggests that mPFC is a feasible candidate for facilitating the associative motor learning under suboptimal learning conditions (Weiss and Disterhoft 1996; Weible et al. 2000; Simon et al. 2005; Oswald et al. 2006, 2009, 2010; Wu et al. 2012, 2015). However, the causal neural pathway through which the mPFC facilitates the associative motor learning under suboptimal learning conditions such as a weak CS (wCS) remains largely unknown. Eyeblink conditioning (EBC) is a unique behavior for investigating the neural mechanisms underlying associative motor learning. Several studies have indicated that the mPFC is required for trace EBC, a more complex type of associative motor learning when there is a temporal gap between the termination of the CS and the onset of the US (Simon et al. 2005; Takehara-Nishiuchi et al. 2005; Oswald et al. 2010; Gruart et al. 2015). Several studies have indicated that the mPFC is required for trace EBC. Our previous work demonstrated that the mPFC plays a critical role in DEC with a soft tone CS (Wu et al. 2012). Moreover, anatomical data show that the mPFC sends substantial synaptic projections to the pontine nucleus (PN), which is the last pre-cerebellar site for convergence of CS-related afferents (Moya et al. 2014). Therefore, we will examine the hypothesis that mPFC and its projection to PN mediate the suboptimal cue (i.e., a weak CS)-induced associative motor learning/memory.

Materials and Methods

Animals

Adult male Sprague Dawley rats, weighing 350–400 g (3–4 months) at the time of virus injection, were individually housed in standard cages on a 12:12 light/dark cycle with free access to food and water *ad libitum*. Behavioral experiments were performed during the light cycle. The room temperature was maintained at 25 ± 1 °C. All animal procedures were approved by the Animal Care Committee of the Third Military Medical University and were performed in accordance with the principles outlined in the National Institutes of Health Guide for the Care and Use of Laboratory Animals.

Virus Injection

Rats were anaesthetized with a mixture of ketamine (100 mg/kg, i.p., Gutian, Fujian, China) and xylazine (9 mg/kg, i.p., Sigma-Aldrich, St. Louis, MO, USA) and fixed in a stereotaxic apparatus (Model 942, David Kopf Instruments, Tujunga, California, USA) as described previously (Wu et al. 2015). The virus was injected using a glass micropipette (tip diameter 10–20 μm) attached to a 5 μL Hamilton microsyringe (51189, Stoelting, Wood Dale, Illinois, USA). The injection rate (0.05 μL/min) was controlled by a stereotaxic microsyringe pump (53311, Stoelting). After injection, the needle was left in place for 5 additional minutes and then slowly withdrawn. For optogenetic inhibition of the bilateral caudal mPFC and of its axon terminals in the PN, rats were bilaterally microinjected with 0.5 μL of pAAV 2/9-CaMKIIα-eNpHR3.0-EYFP [Virus titers: 2.24×10^{13} genome copy (GC)/mL] or pAAV 2/9-CaMKIIα-EYFP (Virus titers: 1.30×10^{13} GC/mL) into both left and right caudal mPFC [anteroposterior (AP) + 1.92 mm from bregma, mediolateral (ML) ± 0.9 mm, dorsoventral (DV) − 3.0 mm] (Figs 2A,B and 4A,B; i.e., ipsilateral and contralateral to the training eye, respectively). Moreover, for optogenetic activation of the bilateral caudal mPFC and of its axon terminals in the PN, rats were bilaterally microinjected with 0.5 μL of pAAV 2/9-CaMKIIα-ChR2(H134R)-mCherry (Virus titers: 1.35×10^{13} GC/mL) or pAAV 2/9-CaMKIIα-mCherry (Virus titers: 1.25×10^{13} GC/mL) into both left and right caudal mPFC (AP + 1.92 mm, ML ± 0.9 mm, DV − 3.0 mm; Figs 3A,B and 5A,B). In addition, previous studies have shown that the mPFC projects bilaterally to the PN, which then projects predominantly to the contralateral cerebellum, and that only the ipsilateral cerebellum (relative to the US presented eye) is required for EBC (Hu et al. 2009; Moya et al. 2014). Thus, for direct optogenetic activation of the PN cell bodies, rats were unilaterally microinjected with 0.5 μL of pAAV 2/9-hSyn-ChR2(H134R)-mCherry (Virus titers: 5.18×10^{12} GC/mL) or pAAV 2/9-hSyn-mCherry (Virus titers: 7.04×10^{12} GC/mL) into the right PN (AP −7.32 mm, ML 0.9 mm, DV −10.0 mm; i.e., contralateral to the training eye) (Fig. 6A,B). These above vectors were obtained from AddGene and packaged by Obio Technology (Shanghai, China).

Immunohistochemistry

To examine the effect of optogenetic stimulation of ChR2-positive cells on endogenous c-Fos expression, 470 nm light stimulation through an optical fiber implanted in the right caudal mPFC (see Supplementary Fig. 8) or the right PN (see Supplementary Fig. 19) of anesthetized rats, which were bilaterally (mPFC) or unilaterally (PN) injected with the virus, was performed for 120 epochs of 250-ms light pulse trains (15 mW/mm^2, 100 Hz, 5 ms pulse duration), separated by 5 s. These rats were then sacrificed 90 min after 470-nm light stimulation. Moreover, 60 min after the last acquisition training, 4 subsets of the behaving rats (i.e., sCS, unpaired group; sCS, paired group; wCS, unpaired group; wCS, paired group) were killed and the brains were immunostained for c-Fos to capture putative memory-related activity patterns in caudal mPFC (Fig. 3F,G).

For immunohistochemistry experiments, rats (including the rats as described above) were injected with an overdose of 10% chloral hydrate (1000 mg/kg, i.p., Kelong, Chengdu, China) and perfused transcardiacally with physiological saline followed by cold 4% paraformaldehyde (PFA; prepared in 0.1 M of phosphate buffer, pH 7.4). The brains were removed from the skull and stored in 4% PFA at 4 °C for 24 h, then transferred to a 30% sucrose solution at 4 °C for 48 h. About 30 μm-thick coronal sections were cut on a freezing microtome (CM3050 S, Leica, Germany) and collected in cold phosphate buffer saline (PBS, 0.01 M, pH 7.4). For immunostaining, each slice was placed in PBST (PBS + 0.3% Triton X-100) with 2% normal bovine serum albumin for 1 h then incubated with primary antibody at 4 °C for 24 h (Mouse anti-CaMKIIα 1:100, C265, Sigma-Aldrich; Mouse Anti-NeuN 1:500, PC213L, Merck; Mouse Anti-GFAP 1:500, G3893, Sigma-Aldrich;

Rabbit anti-c-Fos 1:100, sc-52, Santa Cruz). Slices then underwent 3 wash steps for 10 min each in PBST, followed by 2 h incubation with secondary antibody (Goat anti-mouse conjugated to AlexaFluor568; Goat anti-mouse conjugated to AlexaFluor488; Goat anti-rabbit conjugated to AlexaFluor488, 1:500, Invitrogen). Slices were washed with PBST (once, 10 min) and incubated for 10 min with Hoechst (1:2000, 861405, Sigma-Aldrich), and then underwent 3 more wash steps of 10 min each in PBST, followed by mounting and coverslipping on microscope slides. Confocal fluorescence images were acquired on a Carl Zeiss LSM 780 scanning laser microscope (Germany) using a 10 × air objective or a 40 × oil immersion objective.

Electrophysiological Verification of Optogenetics

The virus-infected rats were anaesthetized by 10% chloral hydrate (400 mg/kg, i.p., Kelong) and their heads were placed in a stereotaxic apparatus (Model 942, David Kopf). An optrode (optrode A) consisting of a fiber-optic cannula (ceramic ferrule: diameter 1.25 mm; optical fiber: 200 μm core diameter, 0.39 NA, FT200EMT, Thorlabs, Newton, New Jersey, USA) with a multi-wire electrode tightly coupled with an optical fiber, with the tips of the electrodes extending approximately 300 μm beyond the tip of optical fiber was used for LED illumination and extracellular or field excitatory postsynaptic potentials (fEPSPs) recordings in the anaesthetized rats. In order to verify the effects of light-emitting diode (LED) illumination of the axon terminals in the PN of eNpHR3.0—expressing mPFC pyramidal neurons, the fEPSPs in PN evoked by electrical stimulation of the mPFC were recorded pre, during and post the PN illumination, respectively (see below, Supplementary Fig. 12). Electrodes were made of 16 individually insulated nichrome wires (17.78 μm inner diameter, 761000, A-M Systems, Sequim, WA, USA), attached to a 20-pin connector. Extracellular and fEPSPs signals were bandpass filtered (0.3–5 kHz and 0.3–500 Hz, respectively), amplified (1000×) using a 16-channel microelectrode amplifier (model 3600, A-M Systems, Sequim, WA, USA) and acquired with a data acquisition system (Powerlab 16/35, ADInstuments, New South Wales, Australia) with a sampling rate of 20 kHz. Spike data were analyzed with NeuroExplorer 4 (MicroBrightField, Williston, VT, USA), a neurophysiological data analysis software. In addition, the other type of optrode (optrode B; ceramic ferrule: diameter 1.25 mm; optical fiber: 200 μm core diameter, 0.39 NA, FT200EMT) consisting of a fiber-optic cannula with 2 recording electrodes (insulated stainless steel wires, 76.2 μm inner diameter, 790900, A-M Systems) directly attached to the optical fiber with the same location of their tips was used for simultaneous LED illumination and for local field potential (LFP) recording in awake behaving rats. The LFP signals were also bandpass filtered (0.3–500 Hz), amplified (1000×) using a 16-channel differential amplifier (model 3500, A-M Systems) and acquired with a data acquisition system (Powerlab 16/35, ADInstuments).

To confirm the physiological effect of LED illumination of eNpHR3.0 on mPFC neuronal activities, an optrode (optrode A, as described above) was slowly lowered to the right caudal mPFC using a hydraulic micromanipulator (PC-5 N, Narishige, Tokyo, Japan) in anesthetized rats transduced in the bilateral caudal mPFC (see Supplementary Fig. 2A) with the pAAV 2/9-CaMKIIα-eNpHR3.0-EYFP virus. The optical fiber was connected to a 590-nm LED (M590F1, Thorlabs, Newton, New Jersey, USA) controlled by a pulse stimulator (Master-9, A.M.P.I., Jerusalem, Israel). The power density of light emitted from the optrode was calibrated to 15 mW/mm^2. After spontaneous firing of neurons was detected, constant 590 nm LED illumination (120 epochs of 250 ms, separated by a variable interval of 20–40 s) reliably suppressed neural activities in a temporally precise, stable, and reversible manner (see Supplementary Fig. 2B,C).

Similarly, for the rats expressing pAAV 2/9-CaMKIIα-ChR2 (H134R)-mCherry in bilaterally mPFC, 470 nm LED illumination (250 ms, 15 mW/mm^2, 100 Hz, 5 ms pulse duration, 120 epochs of 250 ms, separated by a variable interval of 20–40 s) induced reliable spikes in mPFC neurons in head-fixed anesthetized rats (see Supplementary Fig. 9A–C) and robust LFP responses in awake behaving rats (see Supplementary Fig. 9D,E). Note that the graph (see Supplementary Fig. 9D) illustrates an example of the mean value of 120 light-induced LFPs.

To verify the effects of LED illumination of axon terminals of eNpHR3.0—expressing mPFC pyramidal neurons in the PN, anesthetized rats expressing pAAV 2/9-CaMKIIα-eNpHR3.0-EYFP in the bilateral caudal mPFC were implanted with an concentric stimulating electrode aimed at the right caudal mPFC (AP +1.92 mm, ML 0.9 mm, DV −3.0 mm) and with an optrode (optrode A, as described above) aimed at the right PN (AP −7.32 mm, ML 0.9 mm, DV −10.0 mm) using 2 hydraulic micromanipulators (PC-5 N, Narishige; see Supplementary Fig. 12A). fEPSPs were evoked in the right PN by single 50 μs, square, cathodal pulses (stimulus intensities ranged from 50 to 120 μA) applied to the right caudal mPFC pre, during (LED on), and post delivering constant 120 epochs of 250-ms LED illumination (590 nm, 25 mW/mm^2), separated by a variable interval of 20–40 s, to the caudal mPFC axon terminals in the PN. As expected, the slope of the fEPSPs evoked at the right caudal mPFC was significantly decreased by optogenetic illumination of the caudal mPFC axon terminals in the right PN (see Supplementary Fig. 12B,C).

Similarly, for the rats expressing pAAV 2/9-CaMKIIα-ChR2 (H134R)-mCherry in bilaterally mPFC, local spiking activities in the right PN of anesthetized rats (see Supplementary Fig. 15A–C) and robust LFP responses in the right PN of awake behaving rats (see Supplementary Fig. 15D,E) were induced by LED illumination of the caudal mPFC axon terminals in the right PN (470 nm, 25 mW/mm^2, 100 Hz, 5 ms pulse duration, 120 epochs of 250 ms, separated by a variable interval of 20–40 s).

Finally, for the rats expressing pAAV 2/9-hSyn-ChR2-mCherry in the right PN, 470 nm LED illumination (250 ms, 15 mW/mm^2, 100 Hz, 5 ms pulse duration, 120 epochs of 250 ms, separated by a variable interval of 20–40 s) also induced reliable firing of the right PN neurons in anesthetized rats (see Supplementary Fig. 20A–C) and robust LFP responses in the right PN of in awake behaving rats (see Supplementary Fig. 20D,E).

Surgery

All of the rats used for behavior training were anaesthetized with a mixture of ketamine (100 mg/kg, i.p., Gutian, Fujian, China) and xylazine (9 mg/kg, i.p., Sigma-Aldrich) and fixed in a stereotaxic apparatus (Model 942, David Kopf) after virus expression. For delivering the shock US and recording the differential electromyography (EMG) activity of the ipsilateral orbicularis oculi (OO) muscle, rats were implanted with 4 electrodes, made of insulated stainless steel wires (76.2 μm inner diameter, 790900, A-M Systems) in the upper eyelid of the left eye. One pair of electrodes for delivering the shock US was implanted subdermal caudal to the left eye. The second pair of electrodes was implanted into the ipsilateral OO muscle to record its EMG activity. The electrode tips were bent as a hook to facilitate a stable insertion in the upper eyelid (Fig. 1A). Moreover, a bare silver wire (0.1 mm in diameter) was connected to 4 stainless steel skull screws as a ground.

In addition, for optogenetic inhibition or activation of the bilateral caudal mPFC, a dual fiber-optic cannula was (ceramic

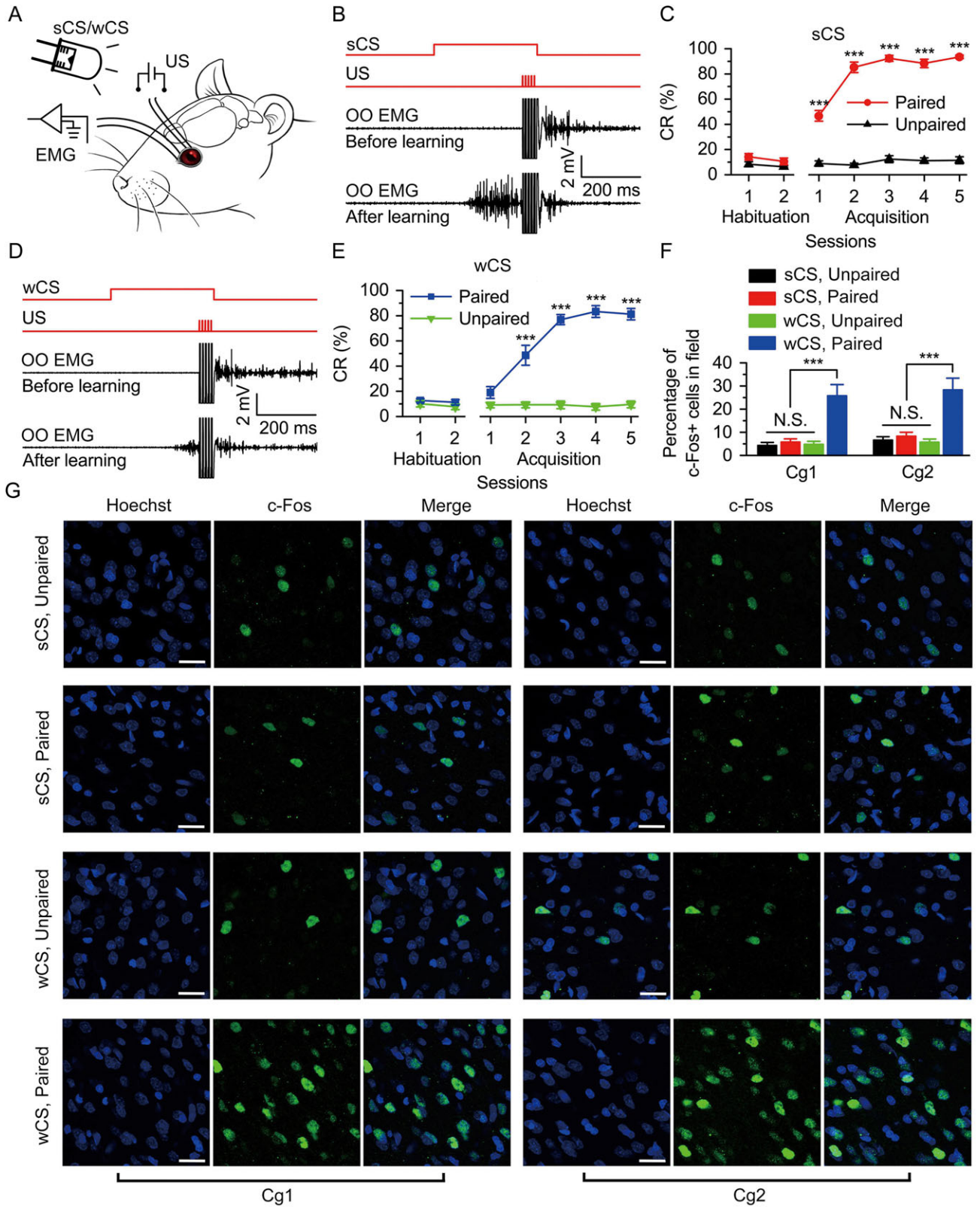

Figure 1. The DEC was supported by both strong CS (sCS) and wCS and the level of c-Fos expression in Cg1 and Cg2 after the last acquisition training. (*A*) Behavioral diagram. For DEC, 2 levels of peripheral light (i.e., 500 nW/mm^2 or 0.5 nW/mm^2) were presented, as sCS and wCS, and 4 electrodes were implanted in the upper left eyelid, 2 for electrical stimulation as the US and the other 2 for recording the EMG activity of the OO muscle. (*B*,*D*) Upper panel: The conditioning paradigm illustrating the timing of the CS and the US. Middle and lower panels: Representative OO EMG before and after learning with the sCS (*B*) or wCS (*D*). (*C*,*E*) Evolution of percentage of conditioned response (CR%) for the sCS (*C*) or wCS (*E*) across 2 habituation and 5 acquisition sessions (*C*: $n = 10$ sCS, paired, $n = 12$ sCS, unpaired; *E*: $n = 9$ wCS, paired, $n = 11$ wCS, unpaired; $^{***}P < 0.001$; 2-way analysis of variance (ANOVA) with repeated measures followed by Tukey post hoc test). (*F*) The percentage of c-Fos-positive cells in Cg1 and Cg2 of 4 groups after the last acquisition training ($n = 6$ each; N.S., not significant, $^{***}P < 0.001$; 1-way ANOVA followed by Tukey post hoc test). (*G*) Representative images of Cg1 and Cg2 following last acquisition training are shown. Scale bars, 20 μm. Data are represented as mean ± standard error of the mean (s.e.m.).

ferrule: diameter 1.25 mm; optical fiber: 200 μm core diameter, 0.39 NA, FT200EMT, Thorlabs) or 2 optrodes (optrode B, as described above) were lowered to 0.3 mm over the virus injection sites in the bilateral caudal mPFC (AP +1.92 mm, ML ±0.9 mm, DV −2.7 mm), respectively (Figs. 2B,E and 3B,E). For muscimol inactivation of the bilateral caudal mPFC, 2 guide cannulae were implanted into the mPFC. Since the tip of the infusion cannula extended 0.3 mm beyond the tip of the guide cannula, the final infusion positions were at following stereotaxic coordinates: AP +1.92 mm, ML ±0.9 mm, and DV −3.0 mm (see Supplementary Fig. 6A,B). For optogenetic inhibition or activation of the caudal mPFC axon terminals in the right PN, and for direct optogenetic activation of the right PN cell bodies, a fiber-optic cannula (for optogenetic inhibition; ceramic ferrule: diameter 1.25 mm; optical fiber: 200 μm core diameter, 0.39 NA, FT200EMT, Thorlabs) or an optrode (for optogenetic activation; optrode B, as described above) was lowered to 0.3 mm over the right PN (AP −7.32 mm, ML 0.9 mm, DV −9.7 mm), respectively (Figs 4B,D, 5B,D, and 6B,E). The wires were connected to an 8-pin mini-strip connector. The mini-strip connector and fiber-optic cannula, optrode, or guide cannula (i.e., headstages) were cemented to the skull

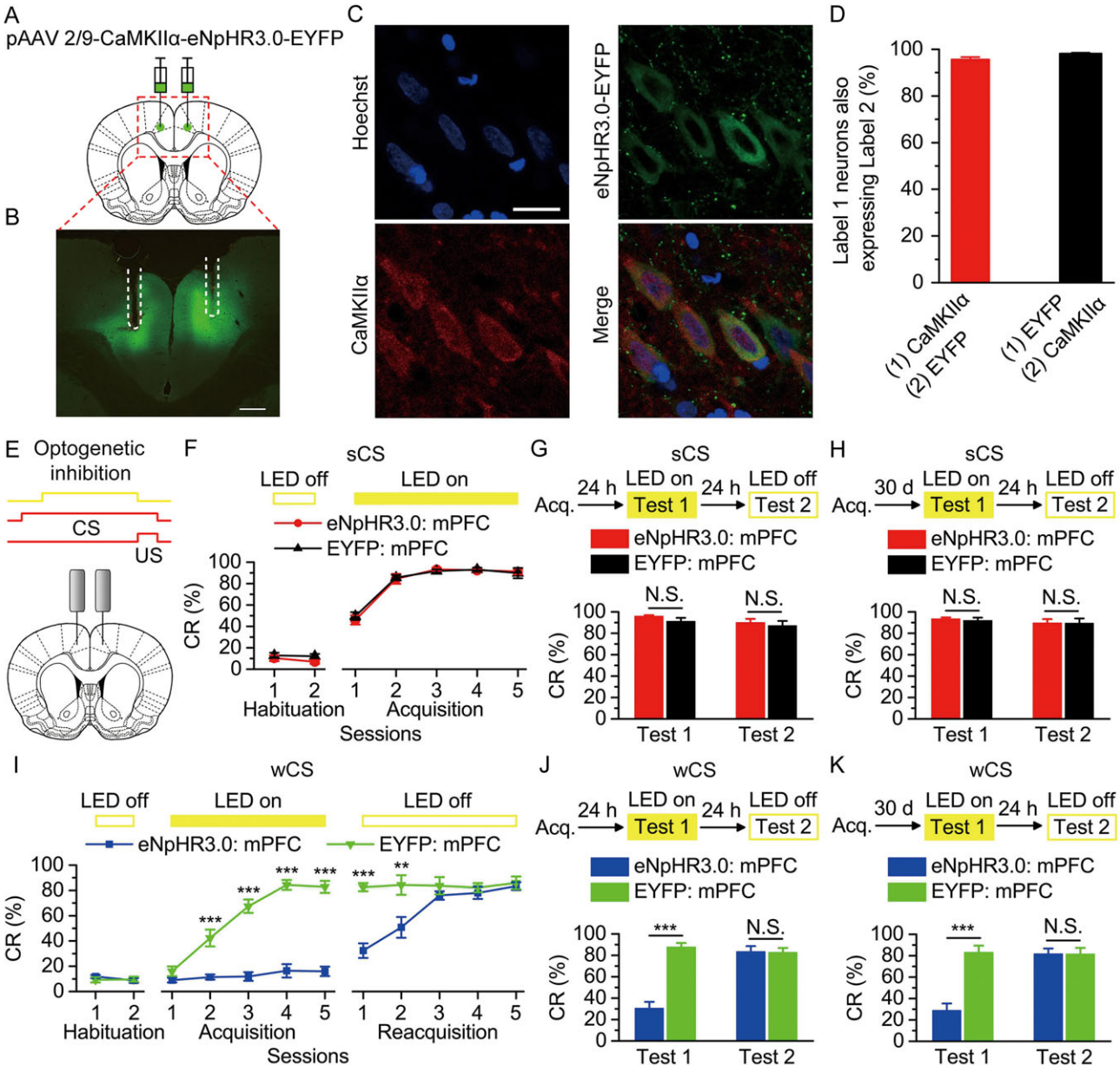

Figure 2. Optogenetic inhibition of the bilateral caudal mPFC impaired the acquisition, recent and remote retrieval of DEC with the wCS, but not of DEC with the sCS. (*A*) Rats were injected with pAAV 2/9-CaMKIIα-eNpHR3.0-EYFP or pAAV 2/9-CaMKIIα-EYFP targeting the bilateral caudal mPFC. (*B*) Example of eNpHR3.0-EYFP expression in the bilateral caudal mPFC. White dashed line: optical fiber position. Scale bar, 500 μm. (*C*) Representative images showing cell-specific eNpHR3.0-EYFP expression (green) in pyramidal neurons (red) in mPFC. Scale bar, 20 μm. (*D*) Statistics of expression in pyramidal neurons (536 cells, from 5 rats). (*E*) Scheme for optical fiber implant site and 590-nm LED illumination pattern to bilateral caudal mPFC during each trial. (*F–K*) Top: Training and illumination phase protocol. Bottom: Effects of mPFC optogenetic inhibition during each trial on CR% of acquisition (*F*: $n = 12$ each; *I*: $n = 12$ eNpHR3.0: mPFC, $n = 10$ EYFP: mPFC), recent retrieval (*G*: $n = 11$ each; *J*: $n = 12$ eNpHR3.0: mPFC, $n = 10$ EYFP: mPFC), and remote retrieval (*H*: $n = 11$ eNpHR3.0: mPFC, $n = 10$ EYFP: mPFC; *K*: $n = 11$ each) of DEC with the sCS or wCS (N.S., not significant, $^{**}P < 0.01$, $^{***}P < 0.001$; 2-way ANOVA with repeated measures followed by Tukey post hoc test or 2-tailed unpaired Student's *t*-test). Data are represented as mean ± s.e.m.

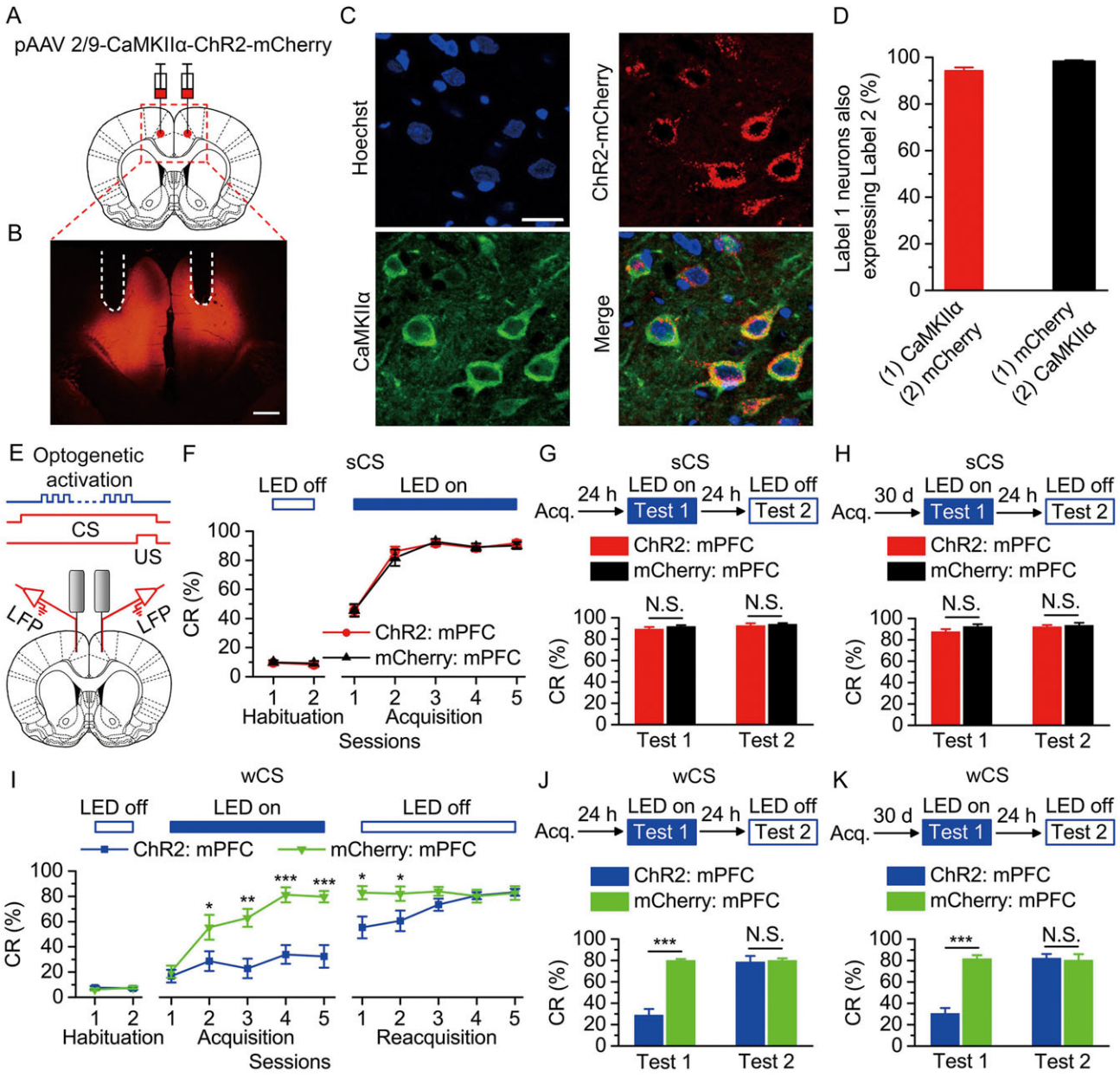

Figure 3. Optogenetic activation of the bilateral caudal mPFC impaired the acquisition, recent and remote retrieval of DEC with the wCS, but not of DEC with the sCS. (*A*) Rats were injected with pAAV 2/9-CaMKIIα-ChR2-mCherry or pAAV 2/9-CaMKIIα-mCherry targeting the bilateral caudal mPFC. (*B*) Example of ChR2-mCherry expression in the bilateral caudal mPFC. White dashed line: optrode position. Scale bar, 500 μm. (*C*) Representative images showing cell-specific ChR2-mCherry expression (red) in pyramidal neurons (green) in mPFC. Scale bar, 20 μm. (*D*) Statistics of expression in pyramidal neurons (497 cells, from 5 rats). (*E*) Scheme for optical fiber implant site and 470-nm LED illumination pattern to bilateral caudal mPFC during each trial. (*F–K*) Top: Training and illumination phase protocol. Bottom: Effects of mPFC optogenetic activation during each trial on CR% of acquisition (*F*: $n = 12$ each; *I*: $n = 12$ ChR2: mPFC, $n = 11$ mCherry: mPFC), recent retrieval (*G*: $n = 11$ each; *J*: $n = 12$ ChR2: mPFC, $n = 9$ for mCherry: mPFC), and remote retrieval (*H*: $n = 11$ each; *K*: $n = 12$ ChR2: mPFC, $n = 11$ mCherry: mPFC) of DEC with the sCS or wCS (N.S., not significant, $^{*}P < 0.01$, $^{**}P < 0.01$, $^{***}P < 0.001$; 2-way ANOVA with repeated measures followed by Tukey post hoc test or 2-tailed unpaired Student's *t*-test). Data are represented as mean ± s.e.m.

with dental cement. After the surgery, the animals were allowed 1 week of recovery.

Behavioral Procedures

Prior to acquisition training, all rats underwent 2 initial 90 min habituation sessions in a plastic box (35 × 25 × 20 cm), housed within a sound- and light-attenuating chamber. For providing a baseline spontaneous blink rate, the EMG activity of the OO muscle of each rat was recorded for 2 habituation sessions in the same way as the conditioning session, except that no stimuli were presented (see below).

The EBC was carried out using a delay paradigm. The CS was a 350-ms, 470-nm peripheral light with either 500 nW/mm^2 or 0.5 nW/mm^2 (i.e., sCS or wCS; tested by a digital optical power and energy meter, PM100D, Thorlabs). The US was a 50-ms periorbital electrical shock (100 Hz, 1 ms pulse duration, square, cathodal pulse), delivered from a stimulus isolator

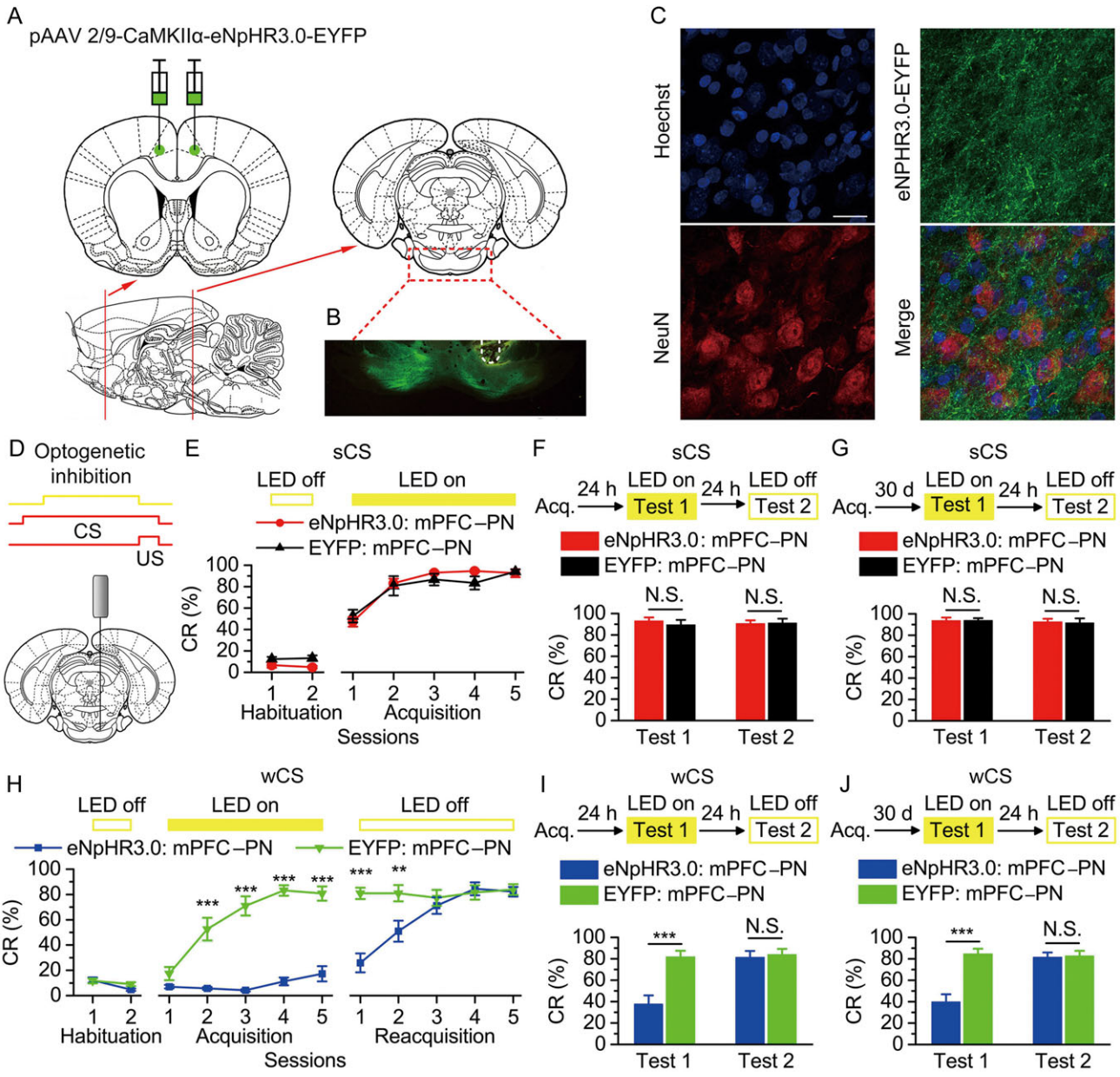

Figure 4. Optogenetic inhibition of the bilateral caudal mPFC axon terminals in the right PN abolished the acquisition, recent and remote retrieval of DEC with the wCS, but not of DEC with the sCS. (*A*) Rats were bilaterally injected with pAAV 2/9-CaMKIIα-eNpHR3.0-EYFP or pAAV 2/9-CaMKIIα-EYFP into the caudal mPFC. (*B*) Example of robust eNpHR3.0-EYFP expression in the axon terminals of mPFC in the PN. White dashed line: optical fiber position. Scale bar, 500 μm. (*C*) Representative images showing images of eNpHR3.0-EYFP-positive axons (green) innervating target neurons in the PN (NeuN, red). Scale bar, 20 μm. (*D*) Coronal schematic of optical fiber implant site and 590-nm LED illumination pattern to the caudal mPFC axon terminals in the PN during each trial. (*E–J*) Top: Training and illumination phase protocol. Bottom: Effects of optogenetic inhibition of mPFC axon terminals in the PN during each trial on CR% of acquisition (*E*: $n = 12$ eNpHR3.0: mPFC–PN, $n = 10$ EYFP: mPFC–PN; *H*: $n = 10$ eNpHR3.0: mPFC–PN, $n = 11$ EYFP: mPFC–PN), recent retrieval (*F*: $n = 12$ eNpHR3.0: mPFC–PN, $n = 11$ EYFP: mPFC–PN; *I*: $n = 9$ eNpHR3.0: mPFC–PN, $n = 10$ EYFP: mPFC–PN), and remote retrieval (*G*: $n = 11$ eNpHR3.0: mPFC–PN, $n = 9$ EYFP: mPFC–PN; *J*: $n = 10$ eNpHR3.0: mPFC–PN, $n = 11$ EYFP: mPFC–PN) of DEC with the sCS or wCS (N.S., not significant, $^{**}P < 0.01$, $^{***}P < 0.001$; 2-way ANOVA with repeated measures followed by Tukey post hoc test or 2-tailed unpaired Student's *t*-test). Data are represented as mean ± s.e.m.

(ISO-Flex, A.M.P.I., Jerusalem, Israel), controlled by a pulse stimulator (Master-9, A.M.P.I.). The intensity of the shock US was carefully calibrated to give the minimal current required to elicit a discrete eyeblink response (2–3 mA). The US intensity was set before the first acquisition session and was not changed during the rest of the experiment. The daily conditioning session (day) consisted of 12 10-trial blocks, each of which comprised 9 CS–US paired trials and 1 CS-alone trial. The trials were separated by a variable inter-trial interval of 20–40 s (with a mean of 30 s). During all of the CS–US paired trials, the CS terminated simultaneously with the US (Fig. 1*B*, *D*). Note that the habituation training was 2 consecutive sessions (days), the acquisition and reacquisition training were 5 consecutive sessions (days), respectively. Moreover, during daily training, each rat was firstly placed in the conditioning box for 30 min without any stimuli, and then received 120 trials of conditioning training (≈ 60 min). Thus, a training session lasted for ≈ 90 min.

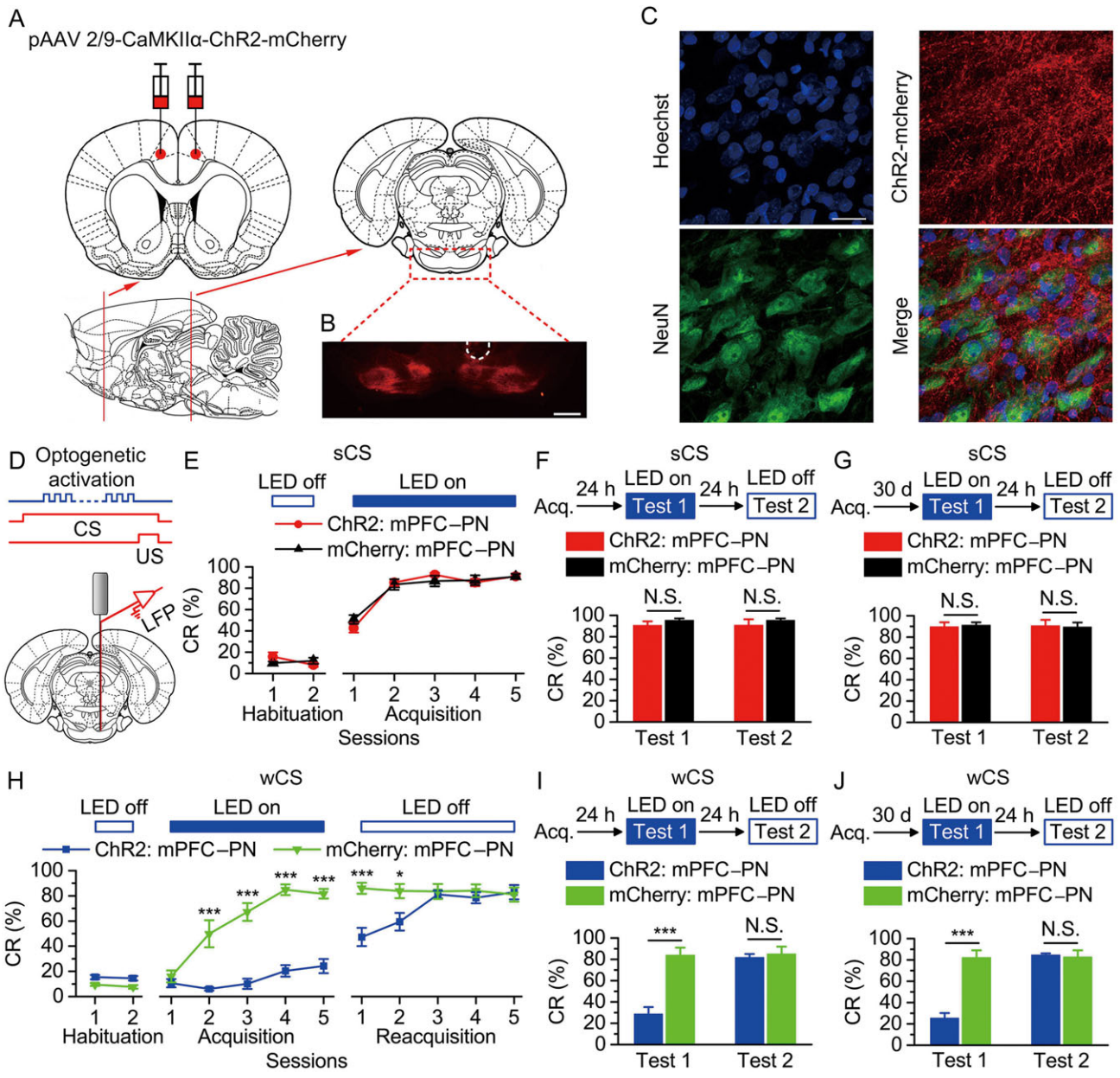

Figure 5. Optogenetic activation of the bilateral caudal mPFC axon terminals in the right PN abolished the acquisition, recent and remote retrieval of DEC with the wCS, but not of DEC with the sCS. (*A*) Rats were bilaterally injected with pAAV 2/9-CaMKIIα-ChR2-mCherry or pAAV 2/9-CaMKIIα-mCherry into the caudal mPFC. (*B*) Example of robust ChR2-mCherry expression in the axon terminals of mPFC in the PN. White dashed line: optrode position. Scale bar, 500 μm. (*C*) Representative images showing images of ChR2-mCherry -positive axons (red) innervating target neurons in the PN (NeuN, green). Scale bar, 20 μm. (*D*) Coronal schematic of optical fiber implant site and 470-nm LED illumination pattern to the caudal mPFC axon terminals in the PN during each trial. (*E–J*) Top: Training and illumination phase protocol. Bottom: Effects of optogenetic activation of mPFC axon terminals in the PN during each trial on CR% of acquisition (E: $n = 10$ each; H: $n = 12$ ChR2: mPFC–PN, $n = 11$ mCherry: mPFC–PN), recent retrieval (F: $n = 11$ ChR2: mPFC–PN, $n = 10$ mCherry: mPFC–PN; I: $n = 12$ ChR2: mPFC–PN, $n = 11$ mCherry: mPFC–PN), and remote retrieval (G: $n = 10$ ChR2: mPFC–PN, $n = 11$ mCherry: mPFC–PN; J: $n = 12$ for ChR2: mPFC–PN, $n = 10$ mCherry: mPFC–PN) of DEC with the sCS or wCS (N.S., not significant, $^{*}P < 0.05$, $^{***}P < 0.001$; 2-way ANOVA with repeated measures followed by Tukey post hoc test or 2-tailed unpaired Student's *t*-test). Data are represented as mean ± s.e.m.

LED Illumination Designs in Optogenetic Manipulations During Behavior

For optogenetic manipulations during behavior, an external optical fiber (200 μm core diameter, 0.39 NA, FT200EMT, Thorlabs), connected to a 470-nm LED (M470F1, Thorlabs) or 590-nm LED (M590F1, Thorlabs), was coupled to an implanted optical fiber (fiber-optic cannula or optrode B, as described above) through a ceramic sleeve. Blue LED (470 nm) or yellow LED (590 nm) illumination was presented to activate ChR2 or eNpHR3.0, respectively, and controlled by a pulse stimulator (Master-9, A.M.P.I.). The power intensity of LED illumination at each fiber tip in brain tissue was measured with a digital optical power and energy meter (PM100D, Thorlabs) and was adjusted to meet experimental requirement. During acquisition and test training with optogenetic manipulations, the LED illumination (250 ms) was applied between 50 ms after the CS onset and the US onset in all trials throughout the training (Figs 2*E* and 4*E*), except for 4 groups in

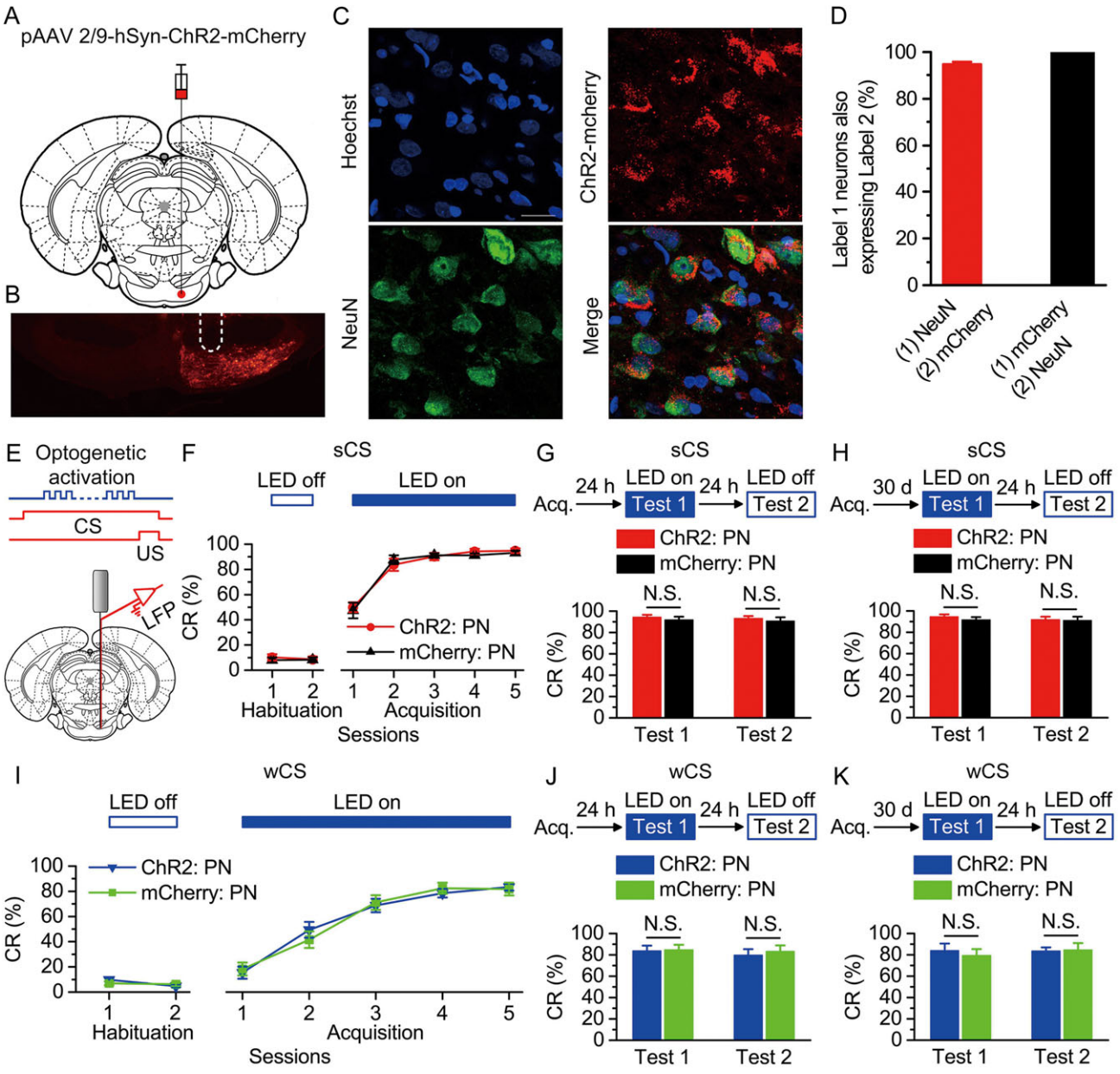

Figure 6. Optogenetic activation of the right PN had no significant effect on the acquisition, recent and remote retrieval of DEC with either the sCS or wCS. (*A*) Rats were injected with pAAV 2/9-hSyn-ChR2-mCherry or pAAV 2/9-hSyn-mCherry targeting the right PN. (*B*) Example of ChR2-mCherry expression in the right PN. White dashed line: optrode position. Scale bar, 500 μm. (*C*) Representative images showing cell-specific ChR2-mCherry expression (red) in neurons (green) of the PN. Scale bar, 20 μm. (*D*) Statistics of expression in neurons (658 cells, from 5 rats). (*E*) Scheme for optical fiber implant site and 470-nm illumination phase pattern to the right PN during each trial. (*F–K*) Top: Training and illumination protocol. Bottom: Effects of optogenetic activation of the right PN during each trial on CR% of acquisition (*F,I*: $n = 12$ ChR2: PN, $n = 11$ mCherry: PN), recent retrieval (*G*: $n = 11$ each; *J*: $n = 10$ each), and remote retrieval (*H*: $n = 12$ ChR2: PN, $n = 11$ mCherry: PN groups; *K*: $n = 9$ ChR2: PN, $n = 11$ mCherry: PN) of DEC with the sCS or wCS (N.S., not significant, 2-way ANOVA with repeated measures or 2-tailed unpaired Student's *t*-test). Data are represented as mean ± s.e.m.

Supplementary Figure 5, in which the LED illumination (350 ms) was applied between 50 ms prior the CS onset and the US onset. In addition, for optogenetic inhibition of the bilateral caudal mPFC or of the caudal mPFC axon terminals in the right PN, the rats received continuous 590-nm LED illumination with 15 mW/mm^2 or 25 mW/mm^2, respectively (Figs 2*F–K* and 4*E–J*). For optogenetic activation of the bilateral caudal mPFC, the right PN cell bodies, or of the caudal mPFC axon terminals in the right PN, the rats received trains of LED illumination pulses (470 nm, 250 ms, 100 Hz, 5 ms pulse duration) with 15 mW/mm^2, 25 mW/mm^2, or 15 mW/mm^2, respectively (Figs 3*F–K*, 5*E–J*, and 6*F–K*).

Pharmacogenetic Inactivation

For pharmacological inactivation of the bilateral caudal mPFC, the $GABA_A$ receptor agonist muscimol (Sigma-Aldrich) was dissolved in artificial cerebrospinal fluid (ACSF) consisting of (in mM): 126 NaCl, 5 KCl, 1.25 NaH_2PO_4, 2 $MgSO_4$, 26 $NaHCO_3$, 2 $CaCl_2$, and 10 glucose (pH 7.35–7.40). The rats were injected with 1.0 μl of muscimol (1.0 mM) or 1.0 μl of ACSF into the bilateral caudal mPFC 30 min before the daily conditioning training (Supplementary Figs 6 and 7). Infusion procedures for each animal included removal of the internal stylet from the guide

cannula, insertion of a stainless steel infusion cannula that extended 0.5 mm beyond the tip of the guide cannula, infusion of the solutions at a constant rate of 0.1 μL/min, removal of the infusion cannula 5 min after the cessation of infusion, and finally reinsertion of the internal stylet (Wu et al. 2012, 2015). The constant injection rate was maintained using a microsyringe pump (53222 V, Stoelting).

Behavioral Data Analysis

EMG activity of the OO muscle and the LFP signals were band-pass filtered (0.1–3 kHz) using an 16-channel differential amplifier (model 3500, A-M Systems) and acquired with a data acquisition system (Powerlab 16/35, ADInstuments) with a sampling rate of 10 kHz.

EMG data were analyzed off-line for quantification of conditioned responses (CRs) with the help of a home-made program. The collected EMG data were full-wave rectified and integrated with a 1-ms time constant. The integrated EMG activity was then calculated to the standard score compared to the mean of the baseline activity for the 0–300 ms before the CS onset in each trial. Thus, the EMG amplitude is given as a percentage of the baseline (100%) averaged EMG amplitude. The mean plus 4 times standard deviation (SD) of the standard EMG activity during the baseline period of each trial was defined as the trial threshold. If the standard EMG amplitude during baseline period exceeded the trial threshold and lasted ≥5 ms, the trial was regarded as a hyperactivity trial and excluded from further analysis. Moreover, a trial was considered to contain the CR if the standard EMG amplitudes exceeded the trial threshold and lasted ≥5 ms during the period of 100–300 ms after the CS onset (i.e., CR period). The percentage of CR (CR%) was defined as the ratio of the number of trials containing the CR to the total number of valid trials. The CR peak amplitude was defined as the maximum amplitude change from the baseline during the CR period. The CR onset latency was defined as the time interval from the CS onset to the time when the standard EMG amplitude first met the criterion for a CR. Moreover, the CR peak latency was defined as the time interval from the CS onset to the peak of the EMG amplitude. Note that only trials containing CRs were selected for analysis of CR peak amplitude, CR onset latency, and CR peak latency. Although the use of EMG could limit the possibility of making inferences about CR timing due to that EMG recordings may be contaminated by activities of larger surrounding muscles like the levator labii superior muscle (Koekkoek et al. 2002), the CR onset latency and CR peak latency based on EMG recording can partially reflect the temporal pattern of the CR. In addition, data from animals were excluded from the analysis under the following circumstances: 1) the headstages dropped out of the skull before the end of the experiments and lead to incomplete recording of the experimental data; 2) the sites of virus injection, or the placements of fiber-optic cannula, optrode, or infusion guide cannula were not in the target areas. Based on the above criterions a total of 41 rats were excluded from the analysis.

Histology

After behavioral experiments, rats were deeply anaesthetized with an overdose of 10% chloral hydrate (1000 mg/kg, i.p., Kelong) and perfused transcardiacally with physiological saline followed by cold 4% PFA (prepared in 0.1 M of phosphate buffer, pH 7.4). The brains were removed from the skull and stored in 4% PFA at 4 °C for 24 h, then transferred to a 30% sucrose solution at 4 °C for 48 h. 40 μm-thick coronal sections were cut on a freezing microtome (CM3050 S, Leica) and collected in cold PBS (0.01 M, pH 7.4). Slices underwent 3 more wash steps of 10 min each in PBST, followed by mounting and coverslipping on microscope slides. The extents of virus expression and placements of fiber-optic cannula, optrode, and infusion guide cannula were carefully checked, and their images were acquired using an Olympus BX53F fluorescence microscope (Japan) using a 2 × air objective.

Statistical Analysis

All of the data were expressed as the mean ± standard error of the mean (s.e.m.). The statistical significance was determined by a 2-tailed unpaired Student's *t*-test, or by an 1-way analysis of variance (ANOVA) followed by Tukey post hoc test, or by a 2-way ANOVA with repeated measures followed by Tukey post hoc test using the SPSS software for the Windows package (v. 18.0). A value of $P < 0.05$ was considered to be statistically significant.

Results

Both the sCS and wCS are Sufficient for Acquisition of DEC

To address the potential role of the mPFC and its functional pathway in modulating associative motor learning, we trained the rats on DEC paradigm with either a strong or weak peripheral light CS (Fig. 1*A*,*B*,*D*). The rats of the 4 groups (i.e., 2 paired with CS and 2 unpaired with CS) showed a very low frequency of spontaneous eyeblink and did not differ significantly from each other during 2 habituation sessions. In contrast, there were progressive increases in the CR% which reach asymptotic values, in the 2 paired groups across acquisition sessions 1–5. This increase was likely due to associative learning, because the 2 unpaired groups did not show an increase in CR percentage across acquisition sessions (Fig. 1*C*,*E*). Moreover, although both sCS and wCS supported the acquisition of the DEC (Fig. 1*C*,*E* and Supplementary Fig. 1), the acquisition of the DEC was faster and reached a little higher asymptote with the sCS than with the wCS, and the CR peak amplitude with the sCS was significantly higher than that with the wCS, suggesting that learning with a suboptimal learning cue is more fragile and therefore more easy to be disrupted.

Higher Density of c-Fos-positive Cells in Cg1 and Cg2 after DEC with the wCS

About 60 min after the last acquisition training, 4 subsets of the above-mentioned behaving rats were killed and the brains were immunostained for c-Fos to capture putative memory-related activity patterns in caudal mPFC. Rats that received DEC with the wCS showed more c-Fos-positive cells in area 1 (Cg1) and area 2 (Cg2) subregions of the anterior cingulate cortex in caudal mPFC of both sides than rats that received DEC with the sCS or an unpaired conditioning (Fig. 1*F*,*G*). These data suggest that the caudal mPFC is activated only during DEC with the wCS but not sCS or unpaired conditioning.

Optogenetic Inactivation of the Caudal mPFC Disrupts the DEC with the wCS, but not with the sCS

Next, to assess the requirement of the caudal mPFC for DEC with only the wCS in rats, we use optogenetic approach to suppress the activities of pyramidal neurons in caudal mPFC in real-time during the DEC. Rats were stereotaxically and bilaterally injected

with plasmid adeno-associated virus (pAAV) encoding either the third-generation chloride pump halorhodopsin fused in-frame to enhanced yellow fluorescent protein (eNpHR3.0-EYFP) or only EYFP under control of the calcium/calmodulin-dependent protein kinase IIα (CaMKIIα) promoter (pAAV-CaMKIIα-eNpHR3.0-EYFP or pAAV-CaMKIIα-EYFP) into the caudal mPFC (Fig. 2*A*,*B*). We then validated the specificity and efficacy of this targeting strategy in vitro. About 95.6 ± 1.0% of CaMKIIα-immunopositive cells expressed eNpHR3.0-EYFP and the promoter also provided high specificity near virus injection sites, because 98.2 ± 0.4% of eNpHR3.0-EYFP-expressing cells were CaMKIIα-immunopositive cells (Fig. 2*C*,*D*). To assess the physiological effects of eNpHR3.0 on mPFC neuronal activity, we performed optrode recordings in anesthetized rats (see Supplementary Fig. 2) and confirmed that continuous illumination of excitatory mPFC neurons with 590-nm LED light inhibited neuronal firing in a temporally precise, stable, and reversible manner (see Supplementary Fig. 2*B*,*C*). To measure the effects of optogenetic inhibition of the caudal mPFC on DEC with a sCS or wCS, A dual fiber-optic cannula was implanted over the bilateral caudal mPFC 4 weeks after virus injection (Fig. 2*B*,*E*). The LED illumination (590 nm, 250 ms, 15 mW/mm^2) was applied between 50 ms after the CS onset and the US onset in all trials throughout the training (Fig. 2*E*). As expected, we found that optogenetic inhibition of the bilateral caudal mPFC, applied within time frame of CS but before US, did not cause significant deficits in the acquisition of DEC with the sCS (Fig. 2*F* and Supplementary Fig. 3*A*–*D*). In contrast, optogenetic inhibition of the caudal mPFC, applied within time frame of CS but before US, significantly impaired the acquisition of DEC with the wCS (Fig. 2*I* and Supplementary Fig. 4*A*–*D*). Importantly, light stimulation of the halorhodopsin of the caudal mPFC, applied between 50 ms after the CS onset and the US onset at 24 h or 30 days after acquisition training, also failed to disrupt the recent and remote retrieval of the DEC with the sCS (Fig. 2*G*,*H* and Supplementary Fig. 3*E*–*L*), but significantly disrupted the recent and remote retrieval of the DEC the wCS (Fig. 2*J*,*K* and Supplementary Fig. 4*E*–*L*). Furthermore, optogenetic inhibition of mPFC starting 50 ms prior to and through the CS also significantly disrupted the acquisition of DEC with the wCS, but not with the sCS (see Supplementary Fig. 5).

In addition, pharmacological inactivation of the caudal mPFC using muscimol, applied at 30 min before animals were tested on the same day (see Methods), did not disturb the acquisition or both the recent and remote retrieval of the DEC with the sCS (see Supplementary Fig. 6), but significantly retarded the acquisition and expression of both the recent and remote retrieval of the DEC with the wCS (see Supplementary Fig. 7).

Optogenetic Activation of the Caudal mPFC Disrupts the DEC with the wCS, but not with the sCS

To further determine the effects of elevating activity of mPFC pyramidal neurons on the DEC with the wCS or sCS, we injected rats with either pAAV-CaMKIIα-ChR2-mCherry or pAAV-CaMKIIα-mCherry into the bilateral caudal mPFC (Fig. 3*A*,*B*). The expression and functionality of ChR2 were also verified by immunohistochemistry and by optrode recording in the anaesthetized and awake behaving rats, respectively (see Supplementary Figs 8 and 9). Similar to the above-mentioned optogenetic inhibition, when the LED illumination (470 nm, 250 ms, 15 mW/mm^2, 100 Hz, 5 ms pulse duration) was performed between 50 ms after the CS onset and the US onset in all trials throughout the training (Fig. 3*E*), we found that optogenetic activation of the bilateral caudal mPFC had no significant effect on the acquisition and both the recent and remote retrieval of the DEC with the sCS (Fig. 3*F*–*H* and Supplementary Fig. 10), but markedly abolished acquisition and retrieval of the DEC with the wCS (Fig. 3*I*–*K* and Supplementary Fig. 11). Taken together, these results suggest that the mPFC selectively modulates the DEC with the wCS (i.e., a relatively more difficult classical motor conditioning), but not the DEC with the sCS (i.e., a standard classical motor learning).

Inhibition of the Caudal mPFC Axon Terminals in the Right PN Abolishes DEC with the wCS, but not with the sCS

Despite the above data showing the selective role of the mPFC in DEC modulation, it is unclear which specific neural pathways are involved in real-time modulation. The mPFC is known to project to several downstream brain regions, e.g., PN, reticulategmental nucleus, dorsal raphe nucleus, dorsal thalamus, hypothalamus, amygdala, and midbrain structures, etc. (Boele et al. 2010; Maeng et al. 2010; Warden et al. 2012; Xu and Sudhof 2013; Moya et al. 2014). Among these regions is the PN, which converges CS-related afferents and then conveys them to the cerebellum via mossy fiber for supporting EBC (Thompson 2005). We further tested the hypothesis that the mPFC selectively modulates the DEC via its substantial projections to the PN. Firstly, to specifically label the mPFC–PN projection, we stereotaxically injected rats with pAAV-CaMKIIα-eNpHR3.0-EYFP or pAAV-CaMKIIα-EYFP into the bilateral caudal mPFC (Fig. 4A), which led to robust NpHR3.0-EYFP or EYFP expression in axon terminals of mPFC pyramidal neuron projections to PN (Fig. 4*B*,*C*). Then, we restrictedly inhibited the activities of mPFC axon terminals at the PN by selectively illuminating this region through a fiber-optic cannula implanted over the right PN (Fig. 4*B*,*D*). In anesthetized rats, in vivo recordings demonstrated that optogenetic inhibition of the caudal mPFC axon terminals in the PN significantly decreased the slope of fEPSPs evoked by the electrical stimulation of the right caudal mPFC (see Supplementary Fig. 12), which indicate the effectiveness of the optogenetic inhibition of mPFC axon terminals in the PN. We then applied LED illumination (590 nm, 250 ms, 25 mW/mm^2) between 50 ms after the CS onset and the US onset in all trials across the training (Fig. 4*D*). When the axon terminals of NpHR3.0-EYFP-expressing caudal mPFC pyramidal neuron projections to PN were optogenetically inhibited, the rats that trained with the sCS did not show effective deficits in acquisition and both the recent and remote retrieval (Fig. 4*E*–*G* and Supplementary Fig. 13), whereas the rats that trained with the wCS showed significant deficits in acquisition and both the recent and remote retrieval (Fig. 4*H*–*J* and Supplementary Fig. 14).

Optogenetic Activation of the Caudal mPFC Axon Terminals in the Right PN Abolishes DEC with the wCS, but not with the sCS

Next, we also examined the effects of optogenetic activation of the caudal mPFC axon terminals in the PN on the DEC with a sCS or wCS. As described above, rats were bilaterally injected with either pAAV-CaMKIIα-ChR2-mCherry or pAAV-CaMKIIα-mCherry into the bilateral caudal mPFC, and after the ChR2-mCherry protein and mCherry protein reached axon terminals in the PN (Fig. 5A–C), an optrode (consisting of 2 recording electrodes glued to a fiber-optic cannula) was placed within the right PN (Fig. 5*B*,*D*). After optogenetic activation of the caudal mPFC axon terminals in the PN, in vivo recording demonstrated

reliable spikes and LFP responses in the PN of anaesthetized and awake behaving rats, respectively (see Supplementary Fig. 15). When the caudal mPFC axon terminals in the PN were LED illuminated (470 nm, 250 ms, 25 mW/mm^2, 100 Hz, 5 ms pulse duration) between 50 ms after the CS onset and the US onset in all trials across the training (Fig. 5*D*), there were no significant deficits in acquisition and both the recent and remote retrieval of the DEC with the sCS in the group of expressing ChR2-mCherry as compared with the mCherry-only group (Fig. 5*E–G* and Supplementary Fig. 16). In contrast, optogenetic activation of the caudal mPFC axon terminals in the PN significantly prevented not only acquisition but also recent and remote retrieval of the DEC with the wCS (Fig. 5*H–J* and Supplementary Fig. 17). Together, these data provide salient evidence that mPFC modulates the DEC with the wCS, but not the sCS, via its downstream projection to pontine nuclei.

Optogenetic Activation of the Right PN have no Significant Effect on the DEC with either the sCS or wCS

Finally, we also sought to test the possibility that the effects of presynaptic optogenetic activation of either the caudal mPFC or its axon terminals in the PN on the DEC would be fully substituted by direct activation of the postsynaptic PN cell bodies. To address this question, we injected rats with pAAV-hSyn-ChR2-mCherry or pAAV-hSyn-mCherry into the right PN (Fig. 6*A,B*). The expression and functionality of ChR2 were also confirmed by immunohistochemistry and optrode recording (Fig. 6*C,D* and Supplementary Figs 18–20), 4 weeks after virus injection and an optrode implantation over the right PN (Fig. 6*B,E*). LED illumination (470 nm, 250 ms, 15 mW/mm^2, 100 Hz, 5 ms pulse duration) was also applied between 50 ms after the CS onset and the US onset in all trials throughout the training (Fig. 6*E*). In contrast to the effects of optogenetic activation of either the caudal mPFC or its axon terminals, optogenetic activation of the PN had no significant effect on the acquisition or both the recent and remote retrieval of either the DEC with the sCS (Fig. 6*F–H* and Supplementary Fig. 21), or the wCS (Fig. 6*I–K* and Supplementary Fig. 22).

Discussion

Here, we have probed the potential role of the mPFC and the causal neural pathways involved in modulating associative motor learning under suboptimal learning conditions by using the optogenetics intervention (inhibition and activation), reversible pharmacological inactivation in awake, freely moving rats and by in vitro c-Fos immunohistochemistry tests. We have shown that both optogenetic inhibition and activation of the bilateral caudal mPFC or its axon terminals at the right PN significantly impaired the acquisition, recent and remote retrieval of DEC with the wCS, but not of DEC with the sCS, and that muscimol inactivation of the bilateral caudal mPFC had similar effects. We have also shown that the associative motor learning with the wCS but not the sCS elicited a significant increase in the number of c-Fos positive cells in Cg1 and Cg2 of both sides. Together, these data clearly demonstrate that the caudal mPFC selectively modulates the associative motor learning with a suboptimal cue via its downstream signaling to the PN. It is of special note that our findings support the notion that the mPFC is not directly involved in the acquisition and retrieval processes of DEC with optimal learning conditions (Powell et al. 2001; McLaughlin et al. 2002; Takehara-Nishiuchi et al. 2005; Leal-Campanario et al. 2007; Kalmbach et al. 2009; Oswald et al. 2010), although the mPFC seems to play a permissive and/or a releasing/depressing role in the DEC expression and is probably involved in the determination of CS–US intervals of an intermediate range during DEC (Leal-Campanario et al. 2013; Caro-Martin et al. 2015).

The significant effects of optogenetic inhibition or activation of mPFC, or its axon terminals at the right PN, on the DEC with the wCS can be explained by the disruption of mPFC's facilitatory effects on the PN-reactivity to the CS signals arriving through the visual projections. It has been reported that CS in the form of electrical shock to the proximal forelimb supported EBC in decerebrated cats only when the CS intensity was increased to a level that it evoked climbing fibers field potentials, suggesting that a critical level of CS intensity is required to form the cerebellar plasticity to support associative motor learning (Hesslow 1994). A critical level of CS salience could be achieved by increasing the CS physical intensity or by cerebrum modulation to enhance CS intensity (Taub and Mintz 2010). Thus, mPFC's facilitatory effects to amplify a low intensity CS may be particularly necessary for associative motor learning with the wCS. It is noticeable that amygdala lesions effectively impaired EBC when the intensity of the tone CS was 65 dB but not when it was 85 dB (Weisz et al. 1992; Lee and Kim 2004; Siegel et al. 2015), suggesting that the amygdala may also serve to enhance the effectiveness of the CS (Boele et al. 2010).

The anomalous findings in this study are that optogenetic activation of mPFC or its PN terminals impairs instead of facilitating DEC with the wCS. One possibility is that the encoding specificity in mPFC neurons is substantially higher thus more apt to be disrupted compared with that in PN neurons. For example, our previous experiment has shown that changing the consistency of the mPFC optogenetic stimulation patterns between acquisition and retrieval significantly affected the DEC performance (Wu et al. 2015). Another consideration is that the mPFC is working in concert with other structure (such as the amygdala) that also sends CS-associated inputs to the mPFC (Lee and Kim 2004; Boele et al. 2010; Siegel et al. 2015), and the mPFC optogenetic activation may be interfering with this converging input. The involvement of amygdala in enhancing the effectiveness of the CS (Boele et al. 2010) suggests the possibility of synergistic effect between mPFC and amygdala to modulate EBC. Other comparable studies showed that a working memory task was impaired not only by mPFC optogenetic inhibition but also by mPFC optogenetic activation during delay period (Liu et al. 2014) and that optogenetic activation of mPFC axons in the brainstem dorsal raphe nucleus affected selection of the active behavioral state (Warden et al. 2012). In order to show a facilitatory role of mPFC or its axon terminals, further detailed studies are needed to find the optimal stimulation parameters like frequency, pulse duration, and intensities, and to dissociate the specific mPFC circuits.

The present study demonstrates that optogenetic activation of the right PN have no modulating effect on the acquisition, recent and remote retrieval of DEC with either the sCS or wCS. It has been reported that probably due to the relatively low encoding specificity in PN, using the PN electrical stimulation CS as a substitute for peripheral CS produced relatively rapid EBC (Steinmetz et al. 1986). Moreover, when PN electrical stimulation CS were transferred to a tone CS after classical conditioning of rabbits, CRs were immediately observed on the first tone CS presentation (Steinmetz 1990). These results strongly suggest that the encoding specificity in PN neurons is substantially low and may not apt to be disrupted. Additionally, optogenetic activation of mPFC or its PN terminals and of the right PN

might activate different sub-networks within the PN thus resulted in distinct outcomes.

Establishment of learning and memory under diverse environment, especially under suboptimal learning conditions is vital for organisms' survival during long evolutionary process. Thus, powerful modulating abilities of learning and memory have been developed. In support, our results provide convincing evidence that the powerful cognitive function of mPFC will be selectively mobilized when necessary to modulate learning and retrieval of wCS-induced DEC, an instantaneous behaved, discrete, and adaptive task. Similarly, several early studies have indicated that the mPFC was implicated in associative learning under other suboptimal learning conditions, including reversal EBC (Chachich and Powell 1998), trace EBC (Han et al. 2003; Takehara-Nishiuchi et al. 2005; Oswald et al. 2010; Siegel and Mauk 2013), and EBC with weak US. It is postulated that mPFC is needed to compare the new CS information with the old in the reversal EBC, and to hold memory traces for significant events during the stimulus-free trace interval of trace EBC to bridge the temporal gap and engage cerebellar learning. (Weiss and Disterhoft 1996; Siegel et al. 2012; Connor and Gould 2016). Indeed, mPFC showed persistent neural activity during the trace EBC (Siegel et al. 2012; Siegel and Mauk 2013), and lesions of the mPFC retarded trace EBC more when the US is a less salient air puff than a more salient periorbital shock (Oswald et al. 2006, 2009, 2010). In this study, by specifically, directly and instantaneously interfere with the neuronal activities of mPFC and its projections to PN, we convincingly demonstrated that the physical intensity of CS determines the involvement or not of mPFC in modulating DEC, and revealed the causal neural pathway underlying this effect. It is noteworthy that selective optogenetic activation of mPFC cells projecting to the brainstem dorsal raphe nucleus induced a profound, rapid and reversible effect on an active behavioral response to challenge (Warden et al. 2012). Furthermore, the central orexinergic system has been also suggested playing a dominant role in modulation of somatic motor behavior when rat is facing a major motor challenge as opposed to during rest and general movements (Zhang et al. 2011; Hu et al. 2015). Taken together, we cautiously suggest, based on a wide range of our results combined with these findings, that during adaptation of the diverse environmental conditions, organisms selectively employ their powerful reserves of brain functions, following the "principle of cognitive economy", to modulate learning and memory under different task loads, which may be of critical significance for the evolution of organisms. In any case, our study may provide an insight into understanding of the mechanisms and the causal neural pathway underlying mPFC's modulation of associative motor learning.

Supplementary Material

Supplementary material are available at *Cerebral Cortex* online.

Notes

We are grateful to Yu Sun for advice on image acquisition and analysis. *Conflict of interest*: None declared.

Funding

This work was supported by grants from the Major State Basic Research Development Program of China (973 program, No. 2014CB541600), the National Natural Science Foundation of China (No. 81171249), Class General Financial Grant from the China Postdoctoral Science Foundation (No. 2014M562592), Special Financial Grant from the China Postdoctoral Science Foundation (No. 2014T81091), and Special Financial Grant from the Chongqing Postdoctoral Science Foundation (No. Xm2015030). QQS is supported by a grant (No. 1R01NS094550) from National Institute of Health (NIH) of the USA.

References

Allen TA, Fortin NJ. 2013. The evolution of episodic memory. Proc Natl Acad Sci USA. 110:10379–10386.

Bellebaum C, Daum I. 2011. Mechanisms of cerebellar involvement in associative learning. Cortex. 47:128–136.

Boele HJ, Koekkoek SK, De Zeeuw CI. 2010. Cerebellar and extracerebellar involvement in mouse eyeblink conditioning: the ACDC model. Front Cell Neurosci. 3:1–19.

Caro-Martin CR, Leal-Campanario R, Sanchez-Campusano R, Delgado-Garcia JM, Gruart A. 2015. A variable oscillator underlies the measurement of time intervals in the rostral medial prefrontal cortex during classical eyeblink conditioning in rabbits. J Neurosci. 35:14809–14821.

Chachich M, Powell DA. 1998. Both medial prefrontal and amygdala central nucleus lesions abolish heart rate classical conditioning, but only prefrontal lesions impair reversal of eyeblink differential conditioning. Neurosci Lett. 257:151–154.

Christian KM, Thompson RF. 2003. Neural substrates of eyeblink conditioning: acquisition and retention. Learn Mem. 10:427–455.

Connor DA, Gould TJ. 2016. The role of working memory and declarative memory in trace conditioning. Neurobiol Learn Mem. 134:193–209.

de Souza Silva MA, Huston JP, Wang AL, Petri D, Chao OY. 2016. Evidence for a specific integrative mechanism for episodic memory mediated by AMPA/kainate receptors in a circuit involving medial prefrontal cortex and hippocampal CA3 region. Cereb Cortex. 26:3000–3009.

Freeman JH. 2015. Cerebellar learning mechanisms. Brain Res. 1621:260–269.

Gigi A, Babai R, Penker A, Hendler T, Korczyn AD. 2010. Prefrontal compensatory mechanism may enable normal semantic memory performance in mild cognitive impairment (MCI). J Neuroimaging. 20:163–168.

Gruart A, Sanchez-Campusano R, Fernandez-Guizan A, Delgado-Garcia JM. 2015. A differential and timed contribution of identified hippocampal synapses to associative learning in mice. Cereb Cortex. 25:2542–2555.

Han CJ, O'Tuathaigh CM, van Trigt L, Quinn JJ, Fanselow MS, Mongeau R, Koch C, Anderson DJ. 2003. Trace but not delay fear conditioning requires attention and the anterior cingulate cortex. Proc Natl Acad Sci USA. 100:13087–13092.

Hesslow G. 1994. Inhibition of classically conditioned eyeblink responses by stimulation of the cerebellar cortex in the decerebrate cat. J Physiol. 476:245–256.

Hu B, Lin X, Huang LS, Yang L, Feng H, Sui JF. 2009. Involvement of the ipsilateral and contralateral cerebellum in the acquisition of unilateral classical eyeblink conditioning in guinea pigs. Acta Pharmacol Sin. 30:141–152.

Hu B, Yang N, Qiao QC, Hu ZA, Zhang J. 2015. Roles of the orexin system in central motor control. Neurosci Biobehav Rev. 49:43–54.

Kalmbach BE, Ohyama T, Kreider JC, Riusech F, Mauk MD. 2009. Interactions between prefrontal cortex and cerebellum revealed by trace eyelid conditioning. Learn Mem. 16:86–95.

Kim JJ, Krupa DJ, Thompson RF. 1998. Inhibitory cerebello-olivary projections and blocking effect in classical conditioning. Science. 279:570–573.

Koekkoek SK, Den Ouden WL, Perry G, Highstein SM, De Zeeuw CI. 2002. Monitoring kinetic and frequency-domain properties of eyelid responses in mice with magnetic distance measurement technique. J Neurophysiol. 88:2124–2133.

Lapish CC, Balaguer-Ballester E, Seamans JK, Phillips AG, Durstewitz D. 2015. Amphetamine exerts dose-dependent changes in prefrontal cortex attractor dynamics during working memory. J Neurosci. 35:10172–10187.

Leal-Campanario R, Delgado-Garcia JM, Gruart A. 2013. The rostral medial prefrontal cortex regulates the expression of conditioned eyelid responses in behaving rabbits. J Neurosci. 33: 4378–4386.

Leal-Campanario R, Fairen A, Delgado-Garcia JM, Gruart A. 2007. Electrical stimulation of the rostral medial prefrontal cortex in rabbits inhibits the expression of conditioned eyelid responses but not their acquisition. Proc Natl Acad Sci USA. 104:11459–11464.

Lee T, Kim JJ. 2004. Differential effects of cerebellar, amygdalar, and hippocampal lesions on classical eyeblink conditioning in rats. J Neurosci. 24:3242–3250.

Lepage M, Ghaffar O, Nyberg L, Tulving E. 2000. Prefrontal cortex and episodic memory retrieval mode. Proc Natl Acad Sci USA. 97:506–511.

Liu D, Gu X, Zhu J, Zhang X, Han Z, Yan W, Cheng Q, Hao J, Fan H, Hou R, et al. 2014. Medial prefrontal activity during delay period contributes to learning of a working memory task. Science. 346:458–463.

Maeng LY, Waddell J, Shors TJ. 2010. The prefrontal cortex communicates with the amygdala to impair learning after acute stress in females but not in males. J Neurosci. 30: 16188–16196.

McLaughlin J, Skaggs H, Churchwell J, Powell DA. 2002. Medial prefrontal cortex and pavlovian conditioning: trace versus delay conditioning. Behav Neurosci. 116:37–47.

Moya MV, Siegel JJ, McCord ED, Kalmbach BE, Dembrow N, Johnston D, Chitwood RA. 2014. Species-specific differences in the medial prefrontal projections to the pons between rat and rabbit. J Comp Neurol. 522:3052–3074.

Oswald B, Knuckley B, Mahan K, Sanders C, Powell DA. 2006. Prefrontal control of trace versus delay eyeblink conditioning: role of the unconditioned stimulus in rabbits (Oryctolagus cuniculus). Behav Neurosci. 120:1033–1042.

Oswald BB, Knuckley B, Mahan K, Sanders C, Powell DA. 2009. Prefrontal control of trace eyeblink conditioning in rabbits (Oryctolagus cuniculus) II: effects of type of unconditioned stimulus (airpuff vs. periorbital shock) and unconditioned stimulus intensity. Physiol Behav. 96:67–72.

Oswald BB, Maddox SA, Tisdale N, Powell DA. 2010. Encoding and retrieval are differentially processed by the anterior cingulate and prelimbic cortices: a study based on trace eyeblink conditioning in the rabbit. Neurobiol Learn Mem. 93:37–45.

Powell DA, Skaggs H, Churchwell J, McLaughlin J. 2001. Posttraining lesions of the medial prefrontal cortex impair performance of pavlovian eyeblink conditioning but have no effect on concomitant heart rate changes in rabbits (Oryctolagus cuniculus). Behav Neurosci. 115:1029–1038.

Prince SE, Tsukiura T, Cabeza R. 2007. Distinguishing the neural correlates of episodic memory encoding and semantic memory retrieval. Psychol Sci. 18:144–151.

Siegel JJ, Kalmbach B, Chitwood RA, Mauk MD. 2012. Persistent activity in a cortical-to-subcortical circuit: bridging the temporal gap in trace eyelid conditioning. J Neurophysiol. 107:50–64.

Siegel JJ, Mauk MD. 2013. Persistent activity in prefrontal cortex during trace eyelid conditioning: dissociating responses that reflect cerebellar output from those that do not. J Neurosci. 33:15272–15284.

Siegel JJ, Taylor W, Gray R, Kalmbach B, Zemelman BV, Desai NS, Johnston D, Chitwood RA. 2015. Trace eyeblink conditioning in mice is dependent upon the dorsal medial prefrontal cortex, cerebellum, and amygdala: behavioral characterization and functional circuitry. eNeuro. 2:1–29.

Simon B, Knuckley B, Churchwell J, Powell DA. 2005. Post-training lesions of the medial prefrontal cortex interfere with subsequent performance of trace eyeblink conditioning. J Neurosci. 25:10740–10746.

Steinmetz JE. 1990. Neuronal activity in the cerebellar interpositus nucleus during classical NM conditioning with a pontine stimulation CS. Psychol Sci. 1:378–382.

Steinmetz JE, Rosen DJ, Chapman PF, Lavond DG, Thompson RF. 1986. Classical conditioning of the rabbit eyelid response with a mossy-fiber stimulation CS: I. Pontine nuclei and middle cerebellar peduncle stimulation. Behav Neurosci. 100:878–887.

Takehara-Nishiuchi K, Kawahara S, Kirino Y. 2005. NMDA receptor-dependent processes in the medial prefrontal cortex are important for acquisition and the early stage of consolidation during trace, but not delay eyeblink conditioning. Learn Mem. 12:606–614.

Taub AH, Mintz M. 2010. Amygdala conditioning modulates sensory input to the cerebellum. Neurobiol Learn Mem. 94: 521–529.

ten Brinke MM, Boele HJ, Spanke JK, Potters JW, Kornysheva K, Wulff P, IJpelaar AC, Koekkoek SK, De Zeeuw CI. 2015. Evolving models of pavlovian conditioning: cerebellar cortical dynamics in awake behaving mice. Cell Rep. 13:1977–1988.

Thompson RF. 2005. In search of memory traces. Annu Rev Psychol. 56:1–23.

Warden MR, Selimbeyoglu A, Mirzabekov JJ, Lo M, Thompson KR, Kim SY, Adhikari A, Tye KM, Frank LM, Deisseroth K. 2012. A prefrontal cortex-brainstem neuronal projection that controls response to behavioural challenge. Nature. 492:428–432.

Weible AP, McEchron MD, Disterhoft JF. 2000. Cortical involvement in acquisition and extinction of trace eyeblink conditioning. Behav Neurosci. 114:1058–1067.

Weiss C, Disterhoft JF. 1996. Eyeblink conditioning, motor control, and the analysis of limbic-cerebellar interactions. Behav Brain Sci. 19:479–481.

Weisz DJ, Harden DG, Xiang Z. 1992. Effects of amygdala lesions on reflex facilitation and conditioned response acquisition during nictitating membrane response conditioning in rabbit. Behav Neurosci. 106:262–273.

Wu GY, Liu GL, Zhang HM, Chen C, Liu SL, Feng H, Sui JF. 2015. Optogenetic stimulation of mPFC pyramidal neurons as a conditioned stimulus supports associative learning in rats. Sci Rep. 5:10065.

Wu GY, Yao J, Zhang LQ, Li X, Fan ZL, Yang Y, Sui JF. 2012. Reevaluating the role of the medial prefrontal cortex in delay eyeblink conditioning. Neurobiol Learn Mem. 97:277–288.

Xu W, Sudhof TC. 2013. A neural circuit for memory specificity and generalization. Science. 339:1290–1295.

Zhang J, Li B, Yu L, He YC, Li HZ, Zhu JN, Wang JJ. 2011. A role for orexin in central vestibular motor control. Neuron. 69: 793–804.